2013 IEEE/RSJ International Conference on
Intelligent Robots and Systems (IROS)
November 3-7, 2013. Tokyo, Japan

Fast 3-D Shape Measurement Using Blink-Dot Projection

Jun Chen, Qingyi Gu, Hao Gao, Tadayoshi Aoyama, Takeshi Takaki, and Idaku Ishii

***Abstract*— We propose a novel dot-pattern-projection three-dimensional (3-D) shape measurement method that can measure 3-D displacements of blink dots projected onto a measured object accurately even when it moves rapidly or is observed from a camera as moving rapidly. In our method, blinking dot patterns, in which each dot changes its size at different timings corresponding to its identification (ID) number, are projected from a projector at a high frame rate. 3-D shapes can be obtained without any miscorrespondence of the projected dots between frames by simultaneous tracking and identification of multiple dots projected onto a measured 3-D object in a camera view. Our method is implemented on a field-programmable gate array (FPGA)-based high-frame-rate (HFR) vision platform that can track and recognize as much as 15×15 blink-dot pattern in a 512×512 image in real time at 1000 fps, synchronized with an HFR projector. We demonstrate the performance of our system by showing real-time 3-D measurement results when our system is mounted on a parallel link manipulator as a sensing head.**

I. INTRODUCTION

In recent times, vision-based three-dimensional (3-D) measurement technologies have been used in many applications such as industrial inspection, object recognition, and robot control. To determine the 3-D positions of multiple points in a camera view, various types of camera-projector systems that project structured light patterns on a measured object at different timings have been developed [1]–[3]. Most of these structured-light systems can compute the 3-D shape information of a measured object at a standstill with triangulation by processing the corresponding images captured by a camera. However, most of these systems used image sensors that follow standard video signals (e.g., NTSC 30 fps or PAL 25 fps), and their accuracy in 3-D measurement decreased when fast-moving objects are observed. For 3-D measurement of fast-moving objects without synchronization errors between multiple light patterns projected at different timings, several one-shot structured light projection methods have also been proposed [4]–[7]. However, most one-shot projection methods have a limited accuracy for 3-D measurement because they assume a local smoothness of an object surface in spatial encoding with one-shot projection.

Assuming a high-frame-rate (HFR) video synchronized with structured light patterns projected from an HFR projector, several approaches have been reported for offline 3-D measurement at thousands of frames per second [8]–[10]. By installing a GPGPU board for parallel processing of a gray-code structured light method [2], Gao et al. have developed a real-time structured light system that can output 512×512 depth images in real time at 500 fps [11]. Compared with standard videos at dozens of frames per second, most of these HFR systems have considerably reduced synchronization errors. However, there are still synchronization errors caused by multiple light patterns projected at different timings when fast-moving objects are observed, depending on the speed of the object and the frame interval of the projection.

For 3-D measurement of moving objects without the assumption of smooth surfaces, multi-spot projection systems have been developed [12], [13], and several HFR systems have been also designed for 3-D measurement in real-time applications [14], [15]. In most of these systems, a stationary multi-spot pattern was projected onto a measured object, and the extracted spots could not be distinguished once they were miscorresponded between frames in exceptional cases such as out-of-camera view or occlusion, because of the no spot identification process. If we could identify the extracted spots in every frame, we could obtain 3-D shapes of moving objects robustly without any miscorrespondence of the extracted spots between frames.

In this study, we develop an HFR blink-dot projection system that can obtain the 3-D information of 15×15 blink dots (maximum) at 1000 fps, synchronized with an HFR projector. Our system can track all the 225 dots in a camera view and extract their identification (ID) numbers by inspecting the temporal changes of their sizes. Section II describes the process flow of our blink-dot projection method. Section III outlines the hardware and software implementation of our method that enables 3-D measurement on $L_X \times L_Y$ blink dots in a 512×512 image in real time at 1000 fps. Section IV presents the results of 3-D measurements conducted when our system was mounted on a parallel link manipulator.

II. BLINK-DOT PROJECTION METHOD

A. Concept

We propose an improved multi-spot projection method (hereafter referred to as the "blink-dot projection method"). This method simultaneously extracts the ID numbers of the multiple spots projected onto a measured object in a camera view for robust and accurate 3-D measurement by projecting several multi-spot patterns at different timings. Figure 1 shows the concept of our blink-dot projection method.

In this study, we focus on the acceleration of multi-blink-dot tracking for HFR 3-D measurement at a thousand of frames per second on the basis of the following concepts:

(a) Multi-dot extraction accelerated by hardware logic

Generally, multi-object extraction requires computation of the order $O(N^2)$, where N^2 is the image size. If we can

J. Chen, Q. Gu, H. Gao, T. Aoyama, T. Takaki, and I. Ishii are with Hiroshima University, Hiroshima 739-8527, Japan (corresponding author (I. Ishii) Tel: +81-82-424-7692; e-mail: j-chen@robotics.hiroshima-u.ac.jp).

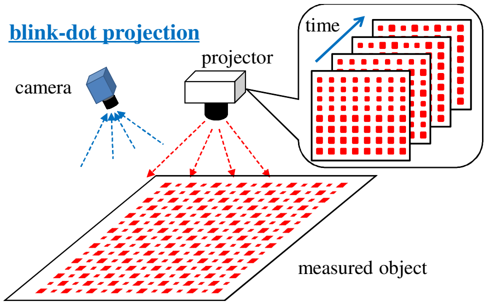

Fig. 1. Blink-dot projection method.

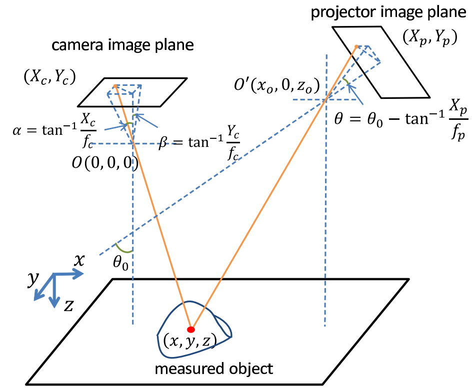

Fig. 2. Geometry of the camera-projector system.

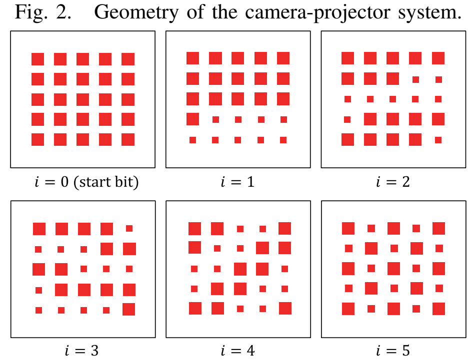

Fig. 3. A blink-dot pattern sequence ($Q = 5$).

implement a multi-object extraction process by parallelized hardware logic as pixel-level computation, multi-dot extraction to localize blink dots projected onto a measured object can be accelerated in our blink-dot projection method. In this study, we accelerate multi-dot extraction by implementing the parallel logic of a cell-based labeling algorithm [17] on a field-programmable gate array (FPGA)-based HFR vision platform. This algorithm is designed to be integrated with hardware logic for fast multi-object feature extraction.

(b) Frame-to-frame correspondence with HFR video

In an HFR video, we assume that the image displacement between frames becomes considerably smaller and allows for a smaller search range for points corresponding to points in the preceding frame. This narrowed search range reduces the computational load of a matching process to correspond the projected dots between frames on the order of $O(L)$, where L is the number of blink dots projected from a projector.

(c) Robust tracking with a blink-dot ID number

The directions of the multiple spot beams projected from a projector are directly determined by inspecting the order of blinks in their time sequences. These multiple spots periodically blink with different sizes at each projection for displaying their ID numbers. Thus, we reduce the miscorrespondences of multiple spots between frames considerably and obtain accurate 3-D shape information, even when there are occlusions or out-of-camera-views. In conventional multi-spot projection methods, the beam directions determined with uncertainty cause serious errors in the 3-D measurement because of triangulation using the beam direction and its pixel position projected onto an image sensor.

We consider our method for the camera-projector system shown in Figure 2. The xyz-coordinate system is defined as the world coordinate system; its origin O is at the optical center of the camera lens. The X_cY_c-coordinate system on the camera image plane is perpendicular to the optical axis, and its origin is located at the intersection with the optical axis of the camera lens. The X_c- and Y_c-axes are parallel to the x- and y-axes, respectively, and the X_cY_c-plane is at a distance f_c from the optical center. The projector is installed in a different direction than the camera; the optical center of the projector lens is $O'(x_0, 0, z_0)$. The optical axis of the projector lens forms an angle θ_0 with respect to the z-axis. The X_pY_p-coordinate system on the projector image plane is perpendicular to the optical axis of the projector lens. The X_pY_p-plane is at a distance f_p from the optical center of the projector lens. The Y_p-axis is parallel to the y-axis. In this study, the X_cY_c- and X_pY_p-coordinate systems are expressed as integer coordinates based on the pixel pitches of the image sensor and projector device, δ_c and δ_p, respectively.

B. Blink-dot pattern to be projected

In this study, the following dot-pattern images $S_i(X_p, Y_p)$ $(i = 0, \cdots, Q)$ are periodically projected from a projector to localize and identify $L_X \times L_Y$ rectangular blink-dot patterns projected onto a measured object:

$$S_i(X_p,Y_p) = \begin{cases} 1 & (|X_p - X_p^{\xi}| \leq w_i^{\xi\eta}, |Y_p - Y_p^{\eta}| \leq w_i^{\xi\eta}) \\ 0 & \text{(otherwise)} \end{cases}. \quad (1)$$

where $Q = \lfloor \log_2 L_X L_Y \rfloor$ is the minimum number of blink-dot patterns that can determine the ID numbers of all $L = L_X L_Y$ dots, and (X_p^{ξ}, Y_p^{η}) is the location of the (ξ, η)-th blink dot in the X_pY_p-space $(\xi = 0, \cdots, L_X - 1, \eta = 0, \cdots, L_Y - 1)$ as follows:

$$(X_p^{\xi}, Y_p^{\eta}) = (D_p\xi + X_p^0, D_p\eta + Y_p^0), \quad (2)$$

where D_p is the interval between the rectangular dots. The ID number $q^{\xi\eta}$ of the (ξ, η)-th dot is determined as follows:

$$q^{\xi\eta} = \eta L_X + \xi \equiv 2^{Q-1} b_{Q-1}^{\xi\eta} + \cdots + 2^0 b_0^{\xi\eta}, \quad (3)$$

where $b_{Q-1}^{\xi\eta}, \cdots, b_0^{\xi\eta}$ express the bits of $q^{\xi\eta}$ in binary notation. The parameter $w_i^{\xi\eta}$ that indicates the size of the (ξ, η)-th dot of $S_i(X_p, Y_p)$ is determined as follows:

$$w_i^{\xi\eta} = \begin{cases} w_L & (i = 0) \\ (w_L - w_S) b_{i-1}^{\xi\eta} + w_S & (i = 1, \cdots, Q) \end{cases}, \quad (4)$$

where $2w_L+1$ and $2w_S+1$ are the edge lengths of the (ξ,η)-th rectangular blink dot when it is ON ($b_i^{\xi\eta}=1$) and OFF ($b_i^{\xi\eta}=0$), respectively. The projection image when $i=0$ is regarded as a start-bit image, in which all of the dots to be projected are large. Otherwise, multiple rectangular dots are periodically blinked with different sizes for displaying their ID numbers. Figure 3 illustrates an example of a 5×5 blink-dot pattern sequence used in our method ($Q=5$).

C. 3-D measurement with blink-dot-identification

After generating the blink-dot pattern sequence described by Eq. (1), the 3-D distribution of blink dots projected onto a measured object is acquired by identifying the blink dots using the following processes. Here, it is assumed that the camera should capture images after a frame cycle time τ, synchronized with the projector.

(a) Projection of blink-dot patterns

The projector projects $(Q+1)$ multi-dot patterns at an interval τ in the order of $S_0(X_p,Y_p)$, $\cdots$, and $S_Q(X_p,Y_p)$.

(b) Image acquisition

A gray-level image of $N\times N$ pixels is captured at time $t=k\tau$ as follows:

$$I_k(X_c,Y_c)=\mathrm{Proj}(S_{k \bmod Q}(X_p,Y_p)), \tag{5}$$

where k indicates the frame number of the captured images.

(c) Binarization

The binary image is obtained by thresholding $I_k(X_c,Y_c)$ with a threshold θ as follows:

$$B_k(X_c,Y_c)=\begin{cases} 1 & (I_k(X_c,Y_c)>\theta) \\ 0 & \text{(otherwise)} \end{cases}. \tag{6}$$

(d) Cell-based labeling

To extract the 0th- and 1st-order moments of L labeled connected components in $B_k(X_c,Y_c)$, we use a cell-based labeling algorithm [17] that reduces the computational complexity in multi-object moment calculations. Based on the additivity in moment calculations, this algorithm can obtain the moments $M_{pq}(O_k^l)$ ($(p,q)=(0,0),(1,0),(0,1)$) for the labeled regions O_k^l ($l=0,\cdots,L-1$) in $B_k(X_c,Y_c)$ by dividing into M^2 cells of $n\times n$ pixels when $N=nM$:

$$M_{pq}(O_k^l)=\sum_{(X_c,Y_c)\in O_k^l} X_c^p\cdot Y_c^q\cdot B_k(X_c,Y_c)\ . \tag{7}$$

(e) Calculation of blink-dot size and location

The size and X_cY_c-position of O_k^l are calculated using their 0th- and 1st-order moments as follows:

$$A(O_k^l)=M_{00}(O_k^l), \tag{8}$$

$$(c_X(O_k^l),c_Y(O_k^l))=\left(\frac{M_{10}(O_k^l)}{M_{00}(O_k^l)},\frac{M_{01}(O_k^l)}{M_{00}(O_k^l)}\right). \tag{9}$$

(f) Determination of the blink state

The blink state of O_k^l is determined by $A(O_k^l)$ as follows:

$$s(O_k^l)=\begin{cases} 1 & (\theta_1^L\le A(O_k^l)<\theta_1^H) \\ 0 & (\theta_0^L\le A(O_k^l)<\theta_0^H) \\ \emptyset & \text{(otherwise)} \end{cases}, \tag{10}$$

where θ_i^L and θ_i^H $(i=0,1)$ are parameters for determining the blink-dot states; 1 and 0 indicate that the blink dot is in the large and small state respectively, and $\emptyset$ indicates that O_k^l does not correspond with any blink dot.

(g) Detection of the start-bit frame

By counting the number of ON-state ($s(O_k^l)=1$) blink dots, the start-bit frame is detected as follows:

$$\tau_k=\begin{cases} 0 & (\sum_{l=0,\cdots,L-1} S(O_k^l)>\theta_S) \\ \tau_{k-1}+1 & \text{(otherwise)} \end{cases}, \tag{11}$$

where τ_k indicates the digit position of the dot ID number.

(h) Frame-to-frame correspondence

Based on the geometrical relationship of the camera-projector system in Figure 2, $L_X\times L_Y$ dot patterns are projected onto L_Y lines in the X_cY_c-plane. These lines are located at regular intervals parallel to the X_c-axis, independent of the 3-D shape of a measured object. Corresponding to the L_Y lines where blink dots are projected, we categorize O_k^l into the following L_Y sets P_k^η ($\eta=0,\cdots,L_Y-1$):

$$P_k^\eta=\{O_k^l:\ |c_Y(O_k^l)-Y_c^\eta|\le\theta_D\}. \tag{12}$$

where $Y_c^\eta=D_c\eta+Y_c^0$ is the Y_c-coordinate of the η-th line. D_c is the interval of the L_Y-lines on the X_cY_c-plane, and θ_D indicates the acceptable deviations of the projected blink dots in the Y_c-direction. Thus, computational complexity for the corresponding multiple extracted regions between frames is reduced by searching the limited number of extracted regions O_{k-1}^l belonging to P_{k-1}^η at the previous frame $k-1$ for the region $O_k^l\in P_k^\eta$ at frame k as follows:

$$T_{k-1}(O_k^l)=\begin{cases} G(O_k^l) & (|c_X(O_k^l)-c_X(G_{k-1}(O_k^l))|<\theta_g) \\ \emptyset & \text{(otherwise)} \end{cases}, \tag{13}$$

$$G_{k-1}(O_k^l)=\underset{O_{k-1}^{l'}\in P_{k-1}^\eta}{\arg\max}\ |c_X(O_k^l)-c_X(O_{k-1}^{l'})|, \tag{14}$$

where $T_{k'}(O_k^l)$ indicates the region at frame k' that corresponds to O_k^l at frame k. θ_g is a threshold to determine the distant pairs of the extracted regions to be discarded, and the number of elements of P_k^η is always less than L_X.

(i) ID number encoding

By checking the blink states of O_k^l among the previous $Q+1$ frames, the ID number $q(O_k^l)$ of O_k^l is encoded based on the start-bit frame as follows:

$$q(O_k^l)=\sum_{i=k-Q}^{k} s(T_i(O_k^l))\cdot 2^{\tau_i}\ . \tag{15}$$

(j) Determination of measurable blink dots

To reduce the number of encoding errors, the measurable state of O_k^l is determined by checking the relationship between its ID number $q(O_k^l)$ and position $(c_X(O_k^l),c_Y(O_k^l))$. We assume that $L_X\times L_Y$ blink-dot patterns are extracted topologically preserved as L dot regions in an image. Then, measurable blink dots are determined with the following measurable ID numbers $q'(O_k^l)$ by checking whether the

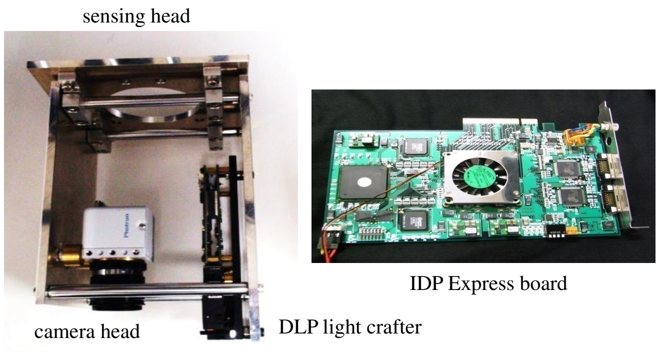

Fig. 4. Overview of the HFR camera-projector system.

encoded ID numbers of L_X extracted regions O_k^l belonging to P_k^η ($\eta = 0, \cdots, L_Y - 1$) are incorrectly located or not:

$$q'(O_k^l) = \begin{cases} \emptyset & (q(O_k^l) \neq \eta L_X + \gamma(O_k^l) \text{ or } s(O_k^l) = \emptyset) \\ q(O_k^l) & \text{(otherwise)} \end{cases}, \quad (16)$$

where $\gamma(O_k^l)$ is the sorting order among the L_X extracted regions belonging to P_k^η when they are sorted in ascending order of their X_c-coordinates $c_X(O_k^l)$.

(h) Triangulation

Using the relationship between $(c_X(O_k^l), c_Y(O_k^l))$ on the X_cY_c-plane and its corresponding point $(X_p^{\xi_k^l}, Y_p^{\eta_k^l})$ on the X_pY_p-plane, the 3-D position (x, y, z) of the (ξ_k^l, η_k^l)-th dot where $q'(O_k^l) \neq \emptyset$ is obtained by solving the following simultaneous equation with a 3×4 camera transform matrix J_c and a 3×4 projector transform matrix J_p:

$$H_c \begin{pmatrix} c_X(O_k^l) \\ c_Y(O_k^l) \\ 1 \end{pmatrix} = J_c \begin{pmatrix} x \\ y \\ z \\ 1 \end{pmatrix}, \quad H_p \begin{pmatrix} X_p^{\xi_k^l} \\ Y_p^{\eta_k^l} \\ 1 \end{pmatrix} = J_c \begin{pmatrix} x \\ y \\ z \\ 1 \end{pmatrix}, \quad (17)$$

where H_c and H_p are parameters, and the matrices J_c and J_p are obtained by prior calibration.

III. System Implementation

A. Configuration

We implemented our blink-dot projection method on an HFR camera-projector system that can process 512 ×512 images in real time at 1000 fps or more. The HFR camera-projector system consists of a high-speed DLP projector (Texas Instruments DLP Light Crafter), the high-speed vision platform IDP Express [16], and a personal computer (PC). Figure 4 shows an overview of the system. The optical center of the projector was at $(x_0, 0, z_0)$ = (52 mm, 0, 15 mm) in the xyz-coordinate system illustrated in Figure 2. The focal lengths of the camera and projector lenses were $f_c = 16$ mm and $f_p = 12.6$ mm, respectively. The optical axis of the projector lens formed an angle of $\theta_0 = 9.1°$ with respect to the z-axis. The projector projected 608×684 images in a 100×178 mm area onto the plane at $z = 342$ mm. The projected pattern was captured as a 512×512 image that corresponds to a 100×100 mm on the plane at $z = 342$ mm.

The DLP Light Crafter is a development kit for high-speed projection, which uses a DMD device; it can project 608×684 binary patterns at 1000 fps or more. Its dimensions and weight are 117×65×23 mm and 170 g, respectively. IDP Express is used as a high-speed image processing system consisting of a camera head and an FPGA processing board (IDP Express board). The camera head can capture 8-bit gray-level images of 512×512 pixels at 2000 fps; its dimensions and weight without a lens are 35×35×34 mm and 90 g, respectively. The IDP Express board is designed for high-speed processing and recording of 512×512 images transferred from the camera head, and it can accelerate image processing algorithms by implementing hardware logic on a user-specified FPGA (Xilinx XC3S5000-4FG900). The IDP Express board has two camera inputs and triggers I/Os for external synchronization. The processed image results could be mapped in the PC memory at 2000 fps or more. The pixel pitches of the image sensor and the DMD device are $\delta_c = 10$ μm and $\delta_p = 7.6$ μm, respectively. The size and dimensions of the prototype sensing head illustrated in Figure 4 are 110×95×170 mm and 995 g, respectively. We use a PC with an ASUSTeK P6T7 mainboard, Intel Core i7 960 3.20 GHz CPU, 3 GB of memory, Windows XP SP3 (32-bit), and two 16-lane PCI-e 2.0 buses.

B. Specifications

Our blink-dot projection method projected several different blink-dot patterns and was implemented on the HFR camera-projector system. For the 608×684 projection images, the location of the $(0, 0)$-th blink dot and the interval between the blink-dots were set to (X_p^0, Y_p^0) = (270, 17) and $D_p = 30$, respectively. The sizes of the large and small dots were manually set depending on the number of blink-dot and measured object in the experiments.

In the implementation of our method described in Subsection II-C, steps (a)–(d) for multi-object moment calculations with a computational complexity of $O(N^2)$ were accelerated by implementing a 4×4-cell-based labeling circuit module on the user-specified FPGA on the IDP Express. However, steps (e)–(h) that require object-level computation with a computational complexity of $O(L)$ were implemented as software on the PC. The 4×4 cell-based labeling circuit module extracted 2048 objects in a 512×512 image and calculated their 0th and 1st moments in real time at 2000 fps. The implementation of the cell-based labeling circuit module was described in detail in [18]. The total execution time of steps (a)–(h) was 0.35 ms, when 15×15 blink dots are used. We confirmed that our HFR camera-projector system executed the blink-dot projection method to extract up to 15×15 blink dots in a 512×512 image and measured their 3-D positions in real time at 1000 fps.

IV. Experiments

To demonstrate the effectiveness of our HFR blink-dot projection system, we conducted experiments involving fast moving scenes. These involved (a) 3-D shape measurement using a fast-moving parallel-link manipulator, and (b) 3-D

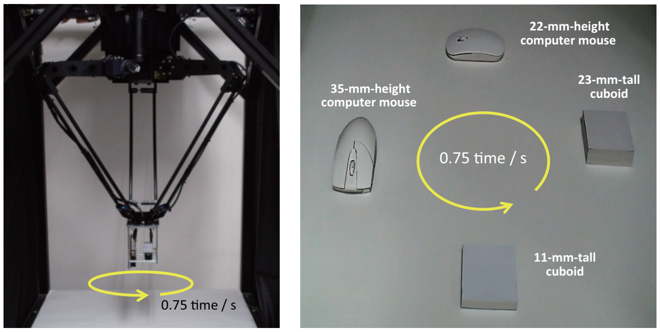

(a) parallel-link manipulator (b) static 3-D scene to be measured

Fig. 5. Experimental environment.

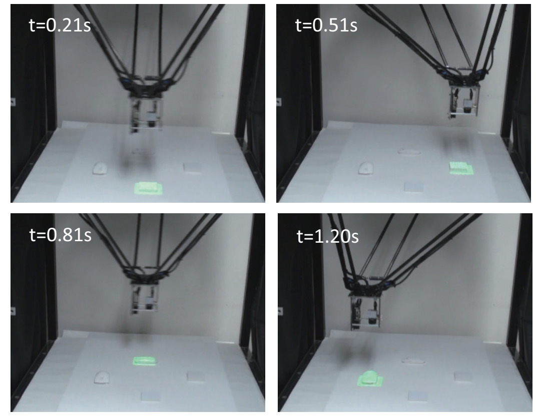

(a) experimental scenes

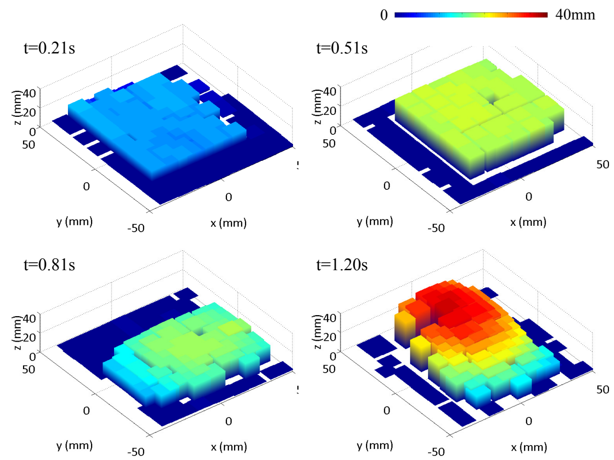

(b) 3-D plots

Fig. 6. 3-D measurement results observed from a fast moving manipulator.

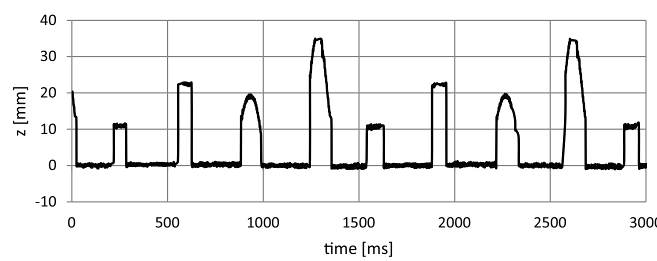

Fig. 7. z coordinate of the (7,7)-th blink-dot.

shape measurement of fast human hand movement. In the experiments, the frame interval and the exposure time of the system were both set to 1 ms and 0.9 ms, respectively.

A. *Static scene observation using a manipulator*

First, we present the 3-D measurement result for a static 3-D scene with height differences when the sensing head of our HFR camera-projector system was mounted on the end of a 3-DOF (degree of freedom) parallel link manipulator. The following parameters were used in the experiment:

– binarization threshold: $\theta = 47$.
– threshold to determine active 4×4 cells: 1 [18].
– number of blink-dot: $L_X = 15$, $L_Y = 15$.
– sizes of large and small dots: $w_L = 4$, $w_S = 2$.
– parameters to determine blink states:
$\theta_1^L = 101$, $\theta_1^H = 300$, $\theta_0^L = 3$, and $\theta_0^H = 100$.
– parameter to determine start-bit frame: $\theta_S = 120$.
– parameters for frame-to-frame correspondence:
$D_c = 30$, $\theta_D = 15$, and $\theta_g = 15$.

Figure 5 shows the experimental setup and the 3-D scene to be observed. In the scene, 23 mm and 11 mm tall cuboids and 35 mm and 20 mm and height computer mice were located on the level plane. In the experiment, the manipulator was controlled to move the sensing head on a circular orbit with radius 20 cm at a cycle time of 1.33 s. The orbit was on the plane at a distance of 342 mm above the level plane. Figure 6 shows (a) the experimental scenes captured using a standard digital video camera, and (b) their color-mapped 3-D plots, which were taken at t = 0.21 s, 0.51 s, 0.81 s and 1.20 s. Here the 3-D plots were corrected based on the depth information measured on the level plane in the same scene. Figure 7 shows the z-coordinate of the (7,7)-th blink dot from t = 0.0–3.0 s. In Figure 6(b), it can be seen that the 3-D shapes of the different height cuboids and computer mouse were correctly measured with 15×15 dots even when the sensing head was quickly moved above the 3-D scene to be measured. In Figure 7, it can be seen that the z-coordinate changed periodically on the order of approximately 11 mm, 23 mm, 20 mm, and 35 cm at a cycle time of 1.33 s, corresponding to the locations of the cuboids and computer mice on the level plane.

B. *Human hand motion*

Next, we present the 3-D measurement result for a human hand moving up and down five times per second 300 mm in front of the sensing head. The following parameters were used in the experiment:

– binarization threshold: $\theta = 38$.
– threshold to determine active 4×4 cells: 2.
– number of blink-dot: $L_X = 10$, $L_Y = 10$.
– sizes of large and small dots: $w_L = 8$, $w_S = 3$.
– parameters to determine blink states:
$\theta_1^L = 151$, $\theta_1^H = 550$, $\theta_0^L = 3$, and $\theta_0^H = 150$.
– parameter to determine start-bit frame: $\theta_S = 51$.
– parameters for frame-to-frame correspondence:

$D_c = 48$, $\theta_D = 24$, and $\theta_g = 24$.

Figure 8 shows (a) the experimental scenes, and (b) their 3-D plots, taken at intervals of 0.06 s for t = 0.21–0.39 s. Figure 9 shows the averaged value of the z-coordinates of the blink-dots projected on the human hand from t = 0.0–1.5 s, excluding the blink-dots projected on the level plane. In Figure 8(b), it can be seen that the 3-D shapes of the human hand were observed, whereas the 10×10 dot resolution was insufficient for a detailed 3-D shape. In Figure 9, the averaged z-coordinate periodically changed with an amplitude of 5 cm at a frequency of 5 Hz, corresponding to the frequency of the human hand's motion.

V. Conclusion

In this study, a blink-dot projection method was proposed for accurate and robust 3-D shape measurement with blink-dot identification, even when a measured object moves rapidly. Our method with 15×15 and 10×10 blink-dot projection was implemented on an HFR camera-projector system. This system measured the 3-D positions of all the blink dots projected onto a measured object by processing 512×512 images in real time at 1000 fps. We verified its effectiveness by conducting experiments with moving objects when our system was mounted on a high-speed manipulator. In the future, we plan to improve our blink-dot projection method for much denser and more robust 3-D shape measurement and to integrate our HFR camera-projector system into a much smaller size for a compact 3-D sensing head of high-speed robot manipulators.

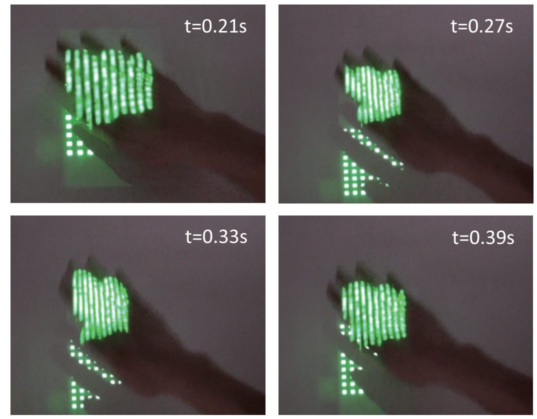

(a) experimental scenes

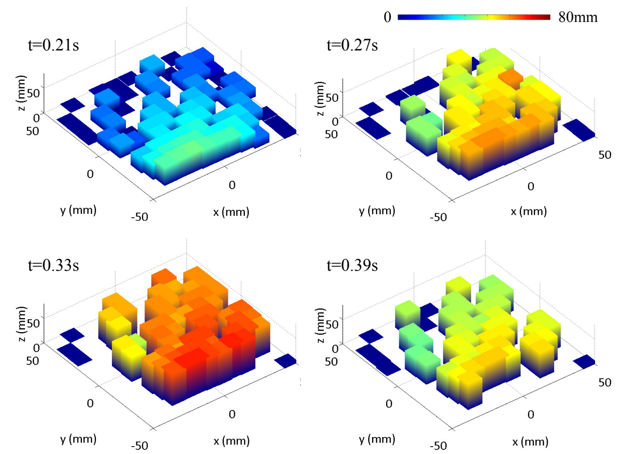

(b) 3-D plots

Fig. 8. 3-D measurement results of a moving human hand.

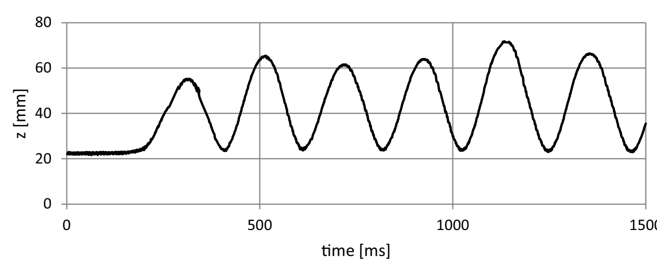

Fig. 9. Averaged z coordinate of a moving human hand.

References

[1] J. L. Posdamer and M. D. Altschuler, "Surface measurement by space-encoded projected beam systems," *Comput. Graph. Image Proc.*, **18**, 1–17, 1982.

[2] S. Inokuchi, K. Sato, and F. Matsuda, "Range imaging system for 3-D object recognition," *Proc. Int. Conf. Pat. Recog.*, 806–808, 1984.

[3] R. L. Valkenburg and A. M. Mcivor, "Accurate 3D measurement using a structured light system," *Opt. Laser. Eng.*, **48**, 149–158, 2010.

[4] P.M. Griffin, L.S. Narasimhan, and S.R. Yee, "Generation of uniquely encoded light patterns for range data acquisition," *Patt. Recog.*, **25**, 609–616, 1992.

[5] J. Pages, J. Salvi, C. Collewet, and J. Forest, "Optimised de Bruijn patterns for one-shot shape acquisition," *Image Vis. Compt.*, **23**, 707–720, 2005.

[6] K. Sakashita, Y. Yagi, R. Sagawa, R. Furukawa, and H. Kawasaki, "A system for capturing textured 3D shapes based on one-shot grid pattern with multi-band camera and infrared projector," *Proc. Int. Conf. 3D Imaging Modeling Processing Visualization and Transmission*, 49–56, 2011.

[7] Microsoft, Xbox 360 Kinect, http://www.xbox.com/en-US/kinect.

[8] I. Ishii, K. Yamamoto, K. Doi, and T. Tsuji, "High-speed 3D image acquisition using coded structured light projection," *Proc. IEEE/RSJ Int. Conf. Intelli. Robot. Sys.*, 925–930, 2007.

[9] J. Takei, S. Kagami, and K. Hashimoto "3,000-fps 3-D shape measurement using a high-speed camera-projector system," *Proc. IEEE/RSJ Int. Conf. Intelli. Robot. Sys.*, 3211–3216, 2007.

[10] S. Zhang, D. Van Der Weide, and J. Oliver, "Superfast phase-shifting method for 3-D shape measurement," *Opt. Exp.*, **18**, 9684–9689, 2010.

[11] H. Gao, T. Takaki, and I. Ishii, "GPU-based real-time structure light 3D scanner at 500 fps," *Proc. SPIE 8437 (SPIE Photonics Europe / Real-Time Image and Video Processing)*, 8437-18, 2012.

[12] K. Nakazawa and C. Suzuki, "Development of 3-D robot vision sensor with fiver grating: Fusion of 2-D intensity image and discrete range image," *Proc. Int. Conf. Industrial Electronics, Control and Instrumentation*, 2368–2372, 1991.

[13] K. Umeda. "A compact range image sensor suitable for robots," *Prof. IEEE Int. Conf. Robot. Automat.*, 3167–3172, 2004.

[14] Y. Watanabe, T. Komura, and M. Ishikawa, "955-fps real-time shape measurement of a moving/deforming object using high-speed vision for numerous-point analysis," *Proc. IEEE Int. Conf. Robot. Automat.*, 3192–3197, 2007.

[15] M. Tateishi, H. Ishiyama and K. Umeda, "A 200 Hz small range image sensor using a multi-spot laser projector," *Proc. IEEE Int. Conf. Robot. Automat.*, 3022–3027 , 2008.

[16] I. Ishii, T. Tatebe, Q. Gu, Y. Moriue, T. Takaki, and K. Tajima, "2000 fps real-time vision system with high-frame-rate video recording," *Proc. IEEE Int. Conf. Robot. Automat.*, 1536–1541, 2010.

[17] Q. Gu, T. Takaki, and I. Ishii, "A fast multi-object extraction algorithm based on cell-based connected components labeling," *IEICE Trans. Info. Syst.*, **E95-D**, 636–645, 2012.

[18] Q. Gu, T. Takaki, and I. Ishii, "Fast FPGA-based multi-object feature extraction," *IEEE Trans. Circuits and Syst. Video Technol.*, **23**, 30–45, 2013.